약학석사 학위논문

항암 치료를 위한

Glycyl-tRNA synthetase 유래 Peptide 개발

Development of Glycyl-tRNA Synthetase-derived Peptide for Cancer Therapy

2017 년 8 월

서울대학교 융합과학기술대학원

분자의학 및 바이오제약학과 의약생명과학전공

박 찬 호

항암 치료를 위한
Glycyl-tRNA synthetase 유래 Peptide 개발

Development of Glycyl-tRNA Synthetase-derived Peptide for Cancer Therapy

지도교수 김 성 훈

이 논문을 약학석사 학위논문으로 제출함

2017 년 7 월

서울대학교 융합과학기술대학원
분자의학 및 바이오제약학과 의약생명과학전공
박 찬 호

박찬호의 약학석사 학위논문을 인준함
2017 년 7 월

위 원 장 김태유 (인)
부 위 원 장 김성훈 (인)
위 원 서영준 (인)

ABSTRACT

Peptide therapeutics is a newly emerging field in cancer therapy. They can be rapidly synthesized and easily modified to fit the drug delivery system needs. Peptides have low toxicity and minimal side effects compared to chemical drugs, which are critical for therapeutic drug development. Glycyl-tRNA synthetase (GRS), a known component of translation, has been previously reported to kill cancer expressing cadherin-6 (CDH-6), also known as K-cadherin, by suppressing ERK signaling and inducing apoptosis. In this study, we analyzed the structure of GRS to determine the active region that binds to CDH6 and critical for cancer cell viability. Only fragment 4 (F4) domain of GRS, 511 to 685 residues, showed binding to CDH6 and induced apoptosis in CDH6-positive cells. Next, we used a protein-protein docking program, HADDOCK (High Ambiguity Driven protein-protein DOCKing), to predict the binding region of F4 to CDH6. Upon this analysis, we predicted single point mutants around N-terminal of F4 would perturb the interface binding. It was shown mutants that lost binding with CDH6 had a decrease in anti-cancer activity against CDH6-positive cancer cells. Double mutants were performed to identify that the region harboring the F535E residue was critical by showing a severe decrease in binding. After confirming the binding domain for GRS and CDH6, a peptide was developed based on these results and analyzed. The peptide showed CDH6 binding and dependent activity in dose-dependent manner through dephosphorylation of ERK signal. Xenograft mouse model showed that peptide suppressed tumor growth only in CDH6-expressing cell line. Our results lead to the discovery of binding site

between GRS with CDH6 and the use of GRS peptide for therapeutic drug development against cancer.

Key words : Glycyl-tRNA synthetase, Peptide, HADDOCK 2.2, Therapeutic drug, Cadherin-6, Mutagenesis, Amino acid

Student ID : 2015-26077

CONTENTS

LIST OF FIGURES

ABBREVIATION LIST

GRS: Glycyl-tRNA synthetase

F2: GRS fragment 2

F4: GRS fragment 4

CDH6: Cadherin-6

PP2A: Phosphatase 2A

FDA: Food and Drug Administration

HADDOCK: High ambiguity Driven protein-protein DOCKing

CRs: Cadherin repeats

NOE: Nuclear Overhasuer Effect

ELISA: Enzyme-linked immunosorbent assay

CCK8: Cell Counting Kit-8

INTRODUCTION

During the past decade, peptides have gained a wide range of application in medicine and biotechnology fields. The estimated peptides and protein market size is more than US $20 billion per year which is about the 10% of the pharmaceutical market (1). In 2012, therapeutics involved peptides have been approved by the Food and Drug Administration (FDA) in the United States for six therapeutic peptides (i.e. lucinactant, peginesatide, pasireotide, carfilzomib, linaclotide, teduglutide) (2, 3). Currently, more than 500 therapeutic peptides are under preclinical trials and approximately 140 peptides are in clinical trials that the numbers of therapeutic peptides are increasing having more than 60 FDA-approved peptides (1, 3).

Aminoacyl- tRNA synthetase (ARSs) are known as enzyme that attach appropriate amino acid onto their tRNA. Non-canonical functions of ARSs have been studied in many different fields having numerous functions beside protein synthesis (4). Several ARSs such as tryptophanyl-tRNA syntethase (WRS) and tyrosyl-tRNA synthetase (YRS) have been reported to act as a secreted cytokines in tumorigenesis and immune responses (5, 6). Glycyl-tRNA synthetase (GRS) also has been reported to have tumor cell killing effect through dephosphorylation of ERK signal in tumor cell. GRS get secreted from macrophage and bind to K-cadherin (CDH6) expressed tumor cell. When GRS binds to CDH6, phosphatase 2A (PP2A) is released and activated PP2A suppresses the ERK signaling by dephosphorlyation of ERK and induces tumor cell apoptosis (7).

Cadherin family, known for cell-cell adhesion molecule, have determined as prognostic marker in neoplasm. Cadherin is a Ca^{2+}- dependent molecule which

mediates the cell-cell binding in a hemophilic manner (8). Classical cadherin is trans-membrane component for the adherence junction (9). For example, E and P-cadherin are involved in adherence junctions in squamous epithelial cells and N-cadherin is associated in fibroblast (10, 11). Cadherin family consist of several cadherin domains and forms rigid rod having calcium ions binding between adjacent cadherin repeats (CRs) (12). GRS binding protein, K-Cadherin (CDH6), is a classic type II cadherin having five extracellular cadherin repeats and each extracellular domain has 27% up to 68% variation. CDH6 and CDH18 shows 54% variation within other cadherin family members having cadherin repeats located near the trans-membrane region, which showed non-shared sequences. This shows that the CDH6 binds to the fourth cadherin repeats in order to induce tumor cell apoptosis (7). Through this identification, GRS specifically binding to CDH6 can be explained.

To find protein-protein interactions, nuclear magnetic resonance (NMR) spectroscopy or x-ray crystallography are mainly used to resolve the determination of protein-protein complexes. Major problem for solving protein-protein complex by NMR requires the information of intermolecular nuclear overhasuer effect (NOE) distance, which has difficulty and long time consuming process (13). High ambiguity driven protein-protein DOCKing (HADDOCK) program is used to find the docking position based on the structure of two proteins. To find the best docking position of two proteins, one protein is fixed and program rotates and translates another protein position calculating the best docking position. Docking position can be predicted using surface complementarities, van der waals repulsion, and electrostatic interaction scoring. Haddock can also be used to find the intermolecular energies using NMR titration data or mutagenesis data (14).

In this study, we have found the GRS fragment (F4) that binds to CDH6 and verified tumor cell apoptosis. Haddock 2.2 was used to predict F4 and CDH6 docking sites and predicted binding residues were driven and validated through mutating binding residues into non-binding residues to see decrease in anti-tumor effect and CDH6 binding. Stringent mutants were designed to confirm the binding resides and through double mutation harboring F535 residue was found to be GRS critical binding site between CDH6. Peptide was designed based on the docking model and showed anti-tumor effect toward CDH6-expressing cancer cell through dephosphorylation of ERK signaling. Peptide showed promising result in xenograft mouse model having tumor suppressing effect toward CDH6-positive cell line. These results suggest that our peptide could be developed as peptide therapeutic drug.

MATERIALS AND METHODS

Cell culture and materials

H460, HCT116, and RENCA cells were grown in RPMI1640 medium and SN12C, MCF7 and HeLa cells were grown in DMEM. Cells were grown with 10% fetal bovine serum with 1% antibiotics at 37°C in a 5% CO_2 incubator.

Cell viability assay

H460, HCT116, MCF7, HeLa, SN12C or RENCA cell line were seeded into 96 well plate, 5000 cells/ml. Proteins were treated after 2 h with 100 µl serum free condition and incubated for 24 h. After 24 h, Cell Counting Kit-8 (CCK-8) assay (Dojindo Laboratories, Kumamoto, Japan) was performed. 10 µl of CCK8 solution was treated and after 1h O.D values was measured using microplate-reader (TECAN, Mannedorf, Swiss) at 450 nm.

Mutagenesis

Followed site-directed mutagenesis kit instructions (Agilent, Santa Clara, CA, USA). Primers were designed accordingly 37 mer with Tm greater than 78°C. For each mutant, 30 ng of F4 mutant DNA, 125 ng of primers, 2.25 mM of dNTP, 10x reaction buffer and 2.5 U/µl Pfu were mixed. Mixing and spinning down, PCR for 95°C for 30 s, then 95°C for 30 s, 55°C for 1 min and 11 min 68°C for 18 cycles were performed. The reaction was then digested with 10U Dpn I for 37°C for 1 hour.

F4 Protein purification (Batch)

Transformation was performed into BL21 competent cell. After spreading into ampicillin plus agar plate, plate was incubated at 37°C overnight. Colony was picked into 3 ml of LB plus ampicillin and up-scaled into 1 L at 37°C. When O.D value

reached 0.6, 1 mM of IPTG (Sigma, St. Louis, MO) was added and incubated overnight at 18°C. At 3500 rpm centrifugation for 30 min and pellet was collected using 7.8 pH buffer. 9 times of sonification were performed and centrifuged for 30 min at 13000 rpm. Supernatant were collected and it was bound to 300 µl of glutathione agarose beads (Thermo, Waltham, MA) for 4 h or overnight. The beads were washed 3 times with 8 ml of PBS and eluted with 500 µl of 40 mM pH 8.0 L-Glutathione reduced (Sigma) for 2 to 4 hr. The protein was dialyzed in PBS-15% glycerol two times, 2 and 6 h or overnight respectively, and harvested. The protein concentrations were measured using protein dye reagent (BioRad, Hercules, CA) at 595 nm spectrometer (Eppendorf, Hamburg, German) and purity was checked by Coomassi staining.

CDH6 Protein purification (column)

Pkk-CDH6-Fc vector (250 µg/100 ml) was transfected into HEK293F cells (2 x 10^6 cells/ml) using Linear PEI (Polysciences, Warrington, PA). Cell was cultured at GIBCO Freestyle™ 293 (TECAN, Mannedorf, Swiss) media for 6 days in 8% CO_2, 37°C. After 6 days of culture, supernatant was collected and centrifuged 2400 rpm for 15 min. Using bottle-top filter (Corning, Kennebunk, ME), supernatant was filter. Using CDH6 (100 ml) supernatant was bound to prewashed 250 µl Protein G agarose beads (Invitrogen, Carlsbad, CA) with 5 ml PBS for three times. The flow through was collected and reloaded to ensure proper binding of CDH6 to beads. The beads were then washed with 5 ml of PBS for a total of three washings. CDH6 was then eluted with 200 µl of 100 nM Glycine pH 2.5 (Affymetrix, Santa Clara, CA) into 20 µl 1M Tris pH 8.8 (Duchefa Biochemie, Haarlem, Netherlands) for neutralization

and this step was repeated four times for a total of six elutions. The protein concentrations were measured using protein dye reagent (BioRad, Hercules, CA) at 595 nm spectrometer (Eppendorf, Hamburg, German) and higher concentrations were pooled. The protein was dialyzed in PBS-15% glycerol two times, 2 and 6 h or overnight respectively, and harvested.

Haddock 2.2 docking program

Crystal structures for CDH6 (pdb id: 3lnd, chain A) and GRS F4 (pdb id: 2pme, residues 256-674) were recovered from the protein data bank. Missing residues were modeled in to both structures using Modeler (15). Energy minimization was carried via the steepest descent and conjugate gradient methods using the Amber 14 molecular modeling package (16). Potential CDH6/F4 complexes were predicted using the protein–protein docking software HADDOCK2.2 (High Ambiguity Driven protein-protein DOCKing) (14). HADDOCK was used to generate 12 poses using rigid body docking, followed by semi-flexible docking with different side-chain rotamers. Each of the 12 poses was evaluated by visual inspection together with buried surface area calculations before and after a short (10 ns) MD simulation using Amber 14. The most stable and biologically realistic complex was thereby selected and used to predict interface mutations that may adversely affect binding.

Pulldown assay

Purified protein 4 μg and 30 μl of glutathione agarose beads (Thermo, Waltham, MA) were incubated for 2 h at 4°C. After three times of PBS washing, CDH6 2 μg was added and incubated for 4 h at 4°C. After the incubation samples were washed with

PBS five times and boiled for 15 min. Sample was analyzed with 10% SDS-PAGE and gel stained with Coomassie, followed by immunoblot analysis using anti-human antibody, 1:10000 (Thermo, Waltham, MA).

Protein stability test

Followed Proteostat Thermal shift stability assay kit instruction (Enzo Life Sience, Farmingdale, NY) 2 μg of protein was added with 2 μl of dye and 10x reaction buffer total volume of 20 μl. Each tube was mixed using pipet and transferred into qRT-PCR plate. Samples were analyzed by Texas Red dye increasing the temperature from 25 to 99°C with 0.3% degree difference in minutes. Experiment was performed using Thermal cycler dice^{TM} Real Time system (Takara, Shiga, Japan) to find melting temperature for each protein and peptide.

Xenograft Mice model

Animal experiments were performed using the University Animal care and committee guidelines at Seoul Nation University. The tumorigenicity of HCT116, SN12C, and RENCA were tested using BALB/c nude female mice. 3 x 10^7 cells were injected to each mouse using a 20-gauge needle and allowed to grow up to 100 mm^3. Tumor growth was checked every 2 days, and when the tumor formation was observed using a caliper to measure tumor size. (Tumor volume was calculated as length x $width^2$ x 0.52). When tumor size reached 100 mm^2, proteins were injected in first day. Tumor weight and size were monitored every 2 days up to 12 days after

injection of proteins. After sacrifices, tumor weights were measured.

RESULTS

GRS derived fragment 4(F4) induces tumor regression by binding to CDH6

Since GRS induces tumor cell apoptosis by binding to CDH6 and blocking ERK signaling, four fragments of GRS were constructed based on domain region maintaining WHEP, catalytic and anti-codon binding domain to see CDH6 binding and anti-cancer effect (7) (Fig. 1A-B). CDH6 binding activity of four fragments were tested through pull-down assay. Among four GRS fragments, only fragment 4 (F4) showed CDH6 binding activity (Fig. 1C). Four fragments were tested for anti-tumor effect using CDH6 expressing cell line (HCT116) and non-CDH6 expressing macrophage (RAW 264.7). GRS fragments had no cytotoxic effect on Raw 264.7 cells, but showed cell killing effect toward HCT116 (Fig. 1D). Only F4 induced tumor apoptosis through CDH6 binding. F4 was next tested to see the anti-cancer effect in xenograft mouse model. HCT116 cells were injected subcutaneously into BALB/C nude mice. After tumors were formed, F2 and F4 were injected. During monitoring period for 15 days, mouse injected with F2 showed increase in tumor size, but mouse injected with F4 maintained the same tumor volume as an initial injection and decreased tumor weight comparing to mouse injected with F2 (Fig. 1E-F). Based on its anti-tumor effect, F4 was used to further investigate CDH6 binding domain

Fragments with truncated N-terminal region of F4 show decrease in anti-tumor activity

Due to seeing anti-cancer effect from F4, N-terminal region was truncated

in order to reduce non-specific binding and conformation changes in F4. Because GRS N-terminal has beta sheet and inserted into the inner area of GRS, three different N-terminal truncated forms of F4 were designed. Using three different length of N-terminal truncated form of F4s (for convenience, GRS-F4-N-terminal truncated formed was names GRS-F4-NT) were designed based on the structure, minimizing the conformation changes and retaining alpha and beta sheet in structure (Fig. 2A). The yield, anti-tumor activity of GRS, F4, GRS-F4-NT1, GRS-F4-NT2, and GRS-F4-NT3 were measured to see which form of F4s is suitable to use to find CDH6 binding domain (Fig. 2B). When the N-terminal regions were truncated, the activity of F4 fragments decreased. Analysis of N-terminal truncated form of F4 on the anti-tumor activity gave a clue on the CDH6 binding site, which may locate from 526 residue to 558 residue. These results suggest that F4 is suitable for finding CDH6 binding domain.

Structure-based docking model predicts the binding site of F4 and CDH6

F4 and CDH6 structure was used from Protein Data Bank (PDB) and the potential interaction domain of CDH6/F4 complex were predicted using the protein-protein docking software HADDOCK2.2. Based on the model run by the program, six residues were selected and point-mutated using opposite trend of amino acid (Fig. 3A). Residues containing arginine, the key of binding (a hotspot residue), was changed to alanine, which has negatively affected in binding. For F539, phenylalanine was mutated into glutamic acid giving negative charge to interrupt the binding. Each mutant was purified and checked for the purity using Coomassie

staining (Fig. 3B). CDH6 binding activity of F4 mutants were measured using ELISA having GRS used as control. Comparing to F4, F539E and E609A mutants had decreased in CDH6 binding activity and also showed decreased anti-tumor activity (Fig. 3C-D).

Confirming active site domain using stringent mutation.

The nearby residues were point-mutated into stringent mutant to increase the disruption in binding with CDH6 for determining the effect on binding and activity. In order to avoid structure conformational changes, stringent mutation was introduced in alpha helix structure and also outer part of F4. Tyrosine, phenylalanine and asparagine were mutated into glutamate or arginine for swapping the charges. Serine was also mutated into tryptophan to introduce bulky amino acid for disrupting the interface (Fig. 4A). Mutated F4 was purified before the experiment checking protein purity through Coomassie staining (Fig. 4B). Using ELISA having GRS as control, F535E showed dramatic decrease in binding and S568W and N570R also showed decrease in CDH6 binding activity (Fig. 4C). F535E residue showed no anti-tumor effects and S568W and N570R residues showed low cancer killing effect (Fig. 4D). Dramatic decrease in binding and anti-tumor activities was observed by introducing stringent mutation in binding domain area. These results suggest that F535 residue, along with S568 and N570 residues are involved in the CDH6 binding site.

Double point mutation showing critical interaction between F4 and CDH6

F535, S568 and N570 residues were used for double point mutation. Structure model showed binding area could be divided into two areas 532 to 549 and 568 to 597. To increase binding disruption, each area was double point mutated including F535, S568 and N570 residues (Fig. 5A). Double mutants and F4 were purified and purity of proteins was checked through coomassie staining (Fig. 5B). ELISA was used to check for CDH6 binding and double mutants having F535 (B-4 and B-5) showed dramatic decrease in binding and mutants with S568 and N570 (A-1) also showed decreased in binding with CDH6 (Fig. 5C). Pull-down assay was performed in order to confirm CDH6 binding. A-1, B-4 and B-5 mutants showed same result with ELISA confirming that mutants associated with F535 and S548/N570 mutants showed dramatic decrease in binding when compared to F4 (Fig. 5D). A-1, B-4 and B-5 showed no anti-cancer effect showing that loss of binding with CDH6 could not induce anti-tumor effect (Fig. 5E).

CDH6 binding and anti-tumor effects of peptide designed based on stringent mutant model

A peptide was next designed to include all six residues identified from stringent mutation studies about the CDH6 binding domain. Peptide also has alpha-helix on both ends to retain stability and conformation having two beta-sheets (Fig. 6A). Peptide showed 80% of the CDH6 binding activity when compared to GRS (Fig. 6B). To see CDH6-dependent activity of peptide, CDH6 and pERK positive

and negative cell lines were tested. Only CDH6 positive cell lines showed decrease in cell viability (Fig. 6C). CDH6 positive and negative renal cancer cell line was used to see peptide dose-dependent activity. Peptide showed activity toward CDH6 expressing cell line, SN12C, in dose-dependent manner (Fig. 6D). To see if the peptide dephosphorylates ERK through CDH6 binding, CDH6 positive cell line, SN12C and negative cell line, RENCA, were used to check dephosphorylation of ERK (Fig. 6E-F). The melting temperature(Tm) was measured using thermal shift assay and peptide showed 53.44°C in melting temperature (Fig. 6G). Thus, we have found that peptide induce cancer cell death through dephosphorylation of ERK in CDH6 dependent manner.

Peptide induces tumor regression in CDH6 positive cancer cell *in vivo* not in CDH6 negative cancer cell

To investigate the peptide effect toward CDH6-positive cell line *in vivo*, we tested peptide in xenograft mouse model using SN12C cells and RENCA cells. CDH6-positive cell line, SN12C, and CDH6-negative cell line were injected into Balb/c nude mice, and tumors were grown until the average size reaches 100mm^3. On day 7 and day 9, PBS and 20 μg of GRS and peptide were directly delivered to the tumors for each group. Mice were harvested on day 17 and photo of mouse was taken along with mouse tumor weight. Compared to control, SN12C xenograft mouse model showed 75% decrease in tumor weight in GRS and peptide injected group, respectively (Fig. 7A-C). Mouse injected with GRS or peptide showed no changes in mouse weight change suggesting lack of toxicity (Fig. 7D). For RENCA

xenograft mouse model, GRS and peptide had no effect toward tumor growth (Fig. 8A-C) and had no toxicity (Fig. 8D).

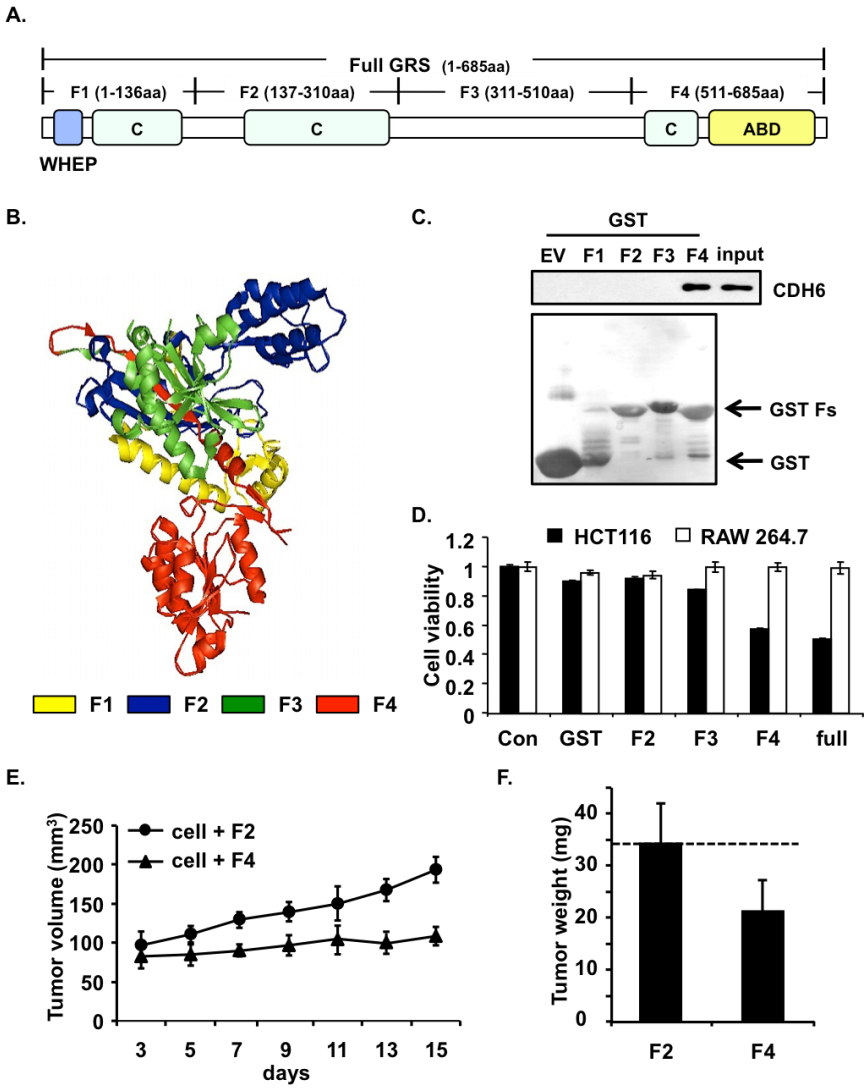

Figure 1. GRS derived fragment 4(F4) induces tumor regression by binding to CDH6

(A) Schematic representation for dividing full length GRS into four fragments sustaining WHEP, Catalytic, and anti-codon binding domain**.**

(B) Each GRS fragment was presented with different color in GRS full-length structure model.

(C) GRS four fragments were purified along with GST-empty vector, CDH6

binding was tested using pull-down assay.

(D) Effect of GRS fragments on cell viability was tested using CDH6 expressing cell line (HCT116) and non-expressing cell line (Raw 264.7).

(E) HCT116 cells were subcutaneously injected into the BALB/c nude mice and grown for 3 days. After tumor formation 100 mm^3, F2 (non-CDH6 binding) and F4 (CDH6 binding) were intra-peritoneal injected 6mpk for four days (n=5 animal/group). Tumor volume was calculated as the longest diameter x the shortest $diameter^2$ x 0.52 for every two days.

(F) Tumor weight of the F2 and F4 treated mice were determined and shown as a bar graph.

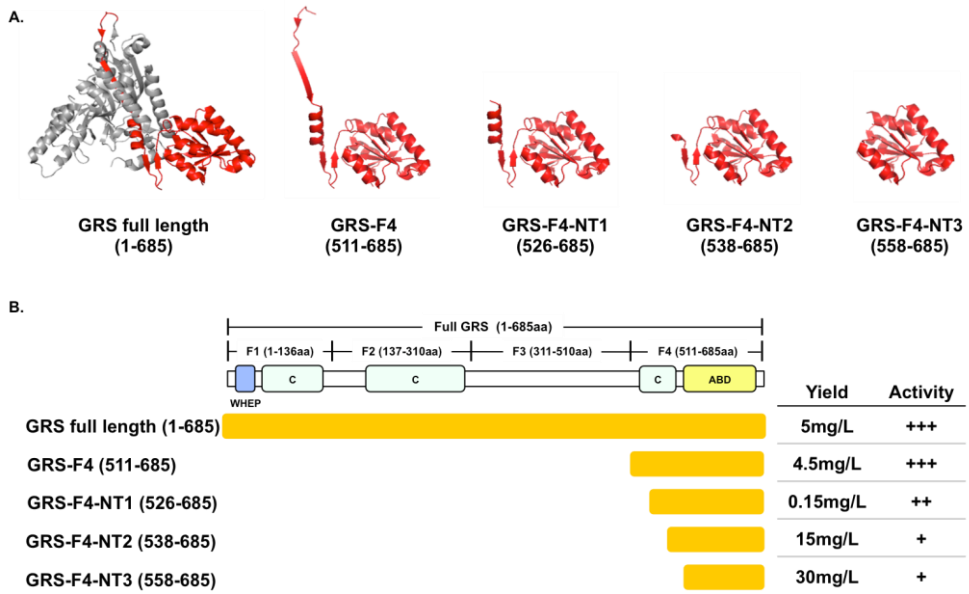

Figure 2. Fragments with truncated N-terminal region of F4 show decrease in anti-tumor activity.

(A) Structure model of each N-terminal truncated F4. Full length GRS, F4, GRS-F4-NT-1, GRS-F4-NT2, and GRS-F4-NT3 were designed.

(B) The effect of GRS, F4 and truncated F4 fragments on cell viability and yield were tested to compare which fragments were suitable to use for finding active domain.

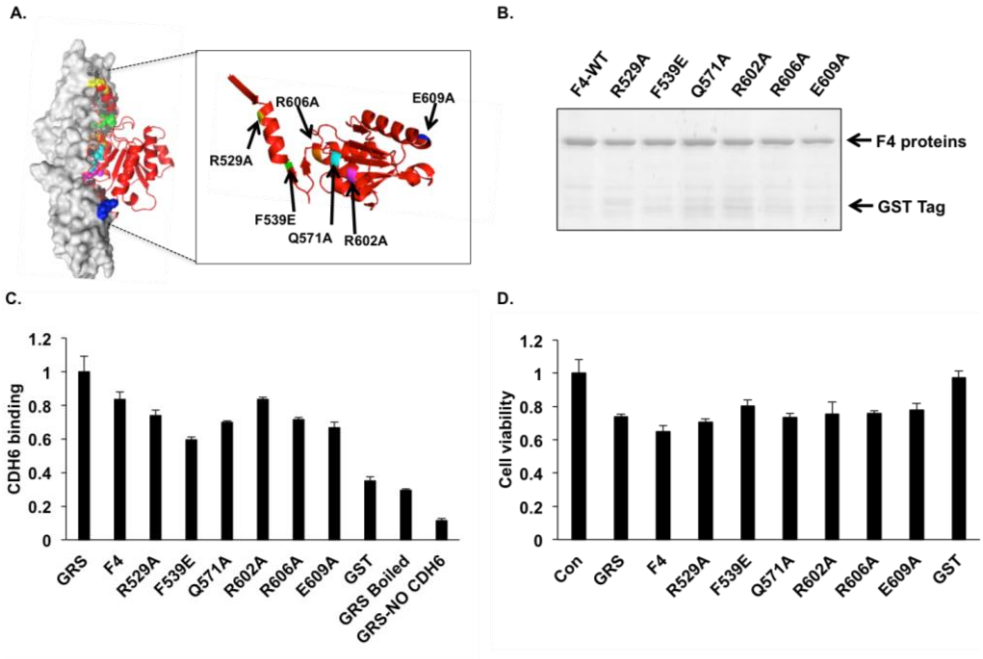

Figure 3. Structure-based docking model predicts the binding site of F4 and CDH6

(A) Crystal structure for CDH6 and GRS F4 were recovered from the protein data bank. Using HADDOCK 2.2, 12 poses of rigid body docking were found, followed by semi-flexible docking with different side-chain rotamers. From 12 poses, Amber 14 was used to finalize docking model based on calculation of buried surface area that has short (10ns) molecular dynamics simulation. Based on docking model, predicted binding site were mutated using opposite trend of amino acid. E, R, Q were mutated into A for negative binding and F was mutated into charged E for disrupt the binding interface.

(B) F4 fragment and other mutants were purified before usage and purity was check using coomassie staining.

(C) Having GRS as positive control, F4 and F4 mutants were coated with 2

μg/ml and CDH6 (2 μg/ml) binding was tested using ELISA.

(D) CDH6 expressing cell line, H460, was treated with 100 nM of F4 and F4 mutants for 24 h and the cell viability was measured by CCK8 assay. GRS 100 nM was used as positive control to induce cell death.

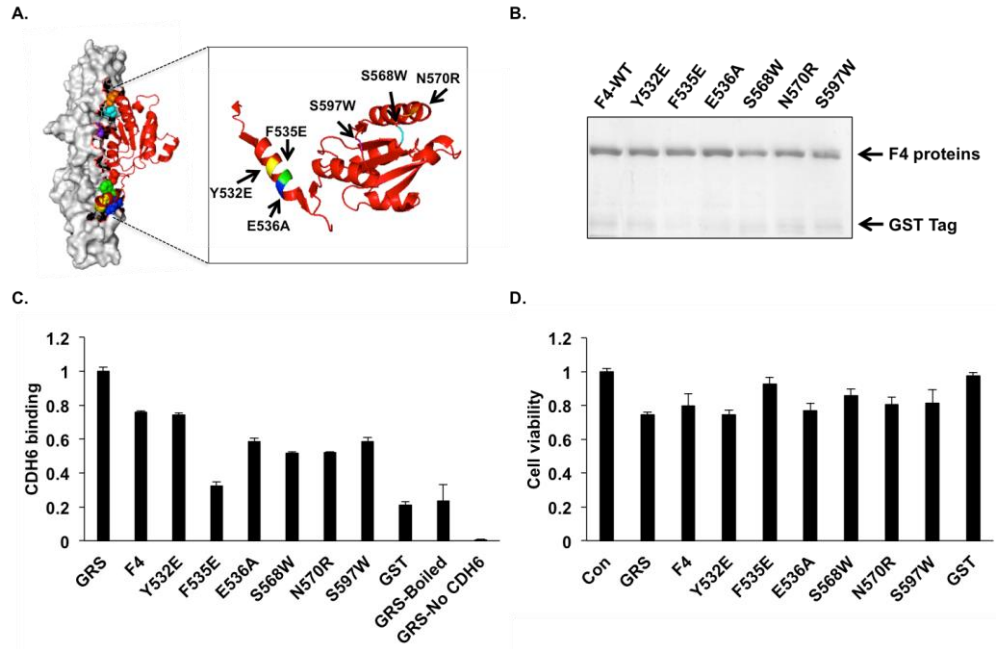

Figure 4. Confirming active site domain using stringent mutation.

(A) Stringent mutation was performed based on docking model. F539 and E609 nearby residues were mutated with stringent mutants. S was mutated into bulky W to disrupt the interface, F and N to R or E for changing into charged amino acid, and E to A for negatively affect binding.

(B) F4 and mutants were purified for experiment and the purity was checked using coomassie staining.

(C) Having GRS as positive control, F4 and F4 mutants were coated with 2 μg/ml and checked CDH6 (2 μg/ml) binding was tested using ELISA.

(D) CDH6 expressing cell line, H460, was treated with 100 nM of F4 and F4 mutants for 24 h and the cell viability was measured by CCK8 assay. GRS 100 nM was used as positive control to induce cell death.

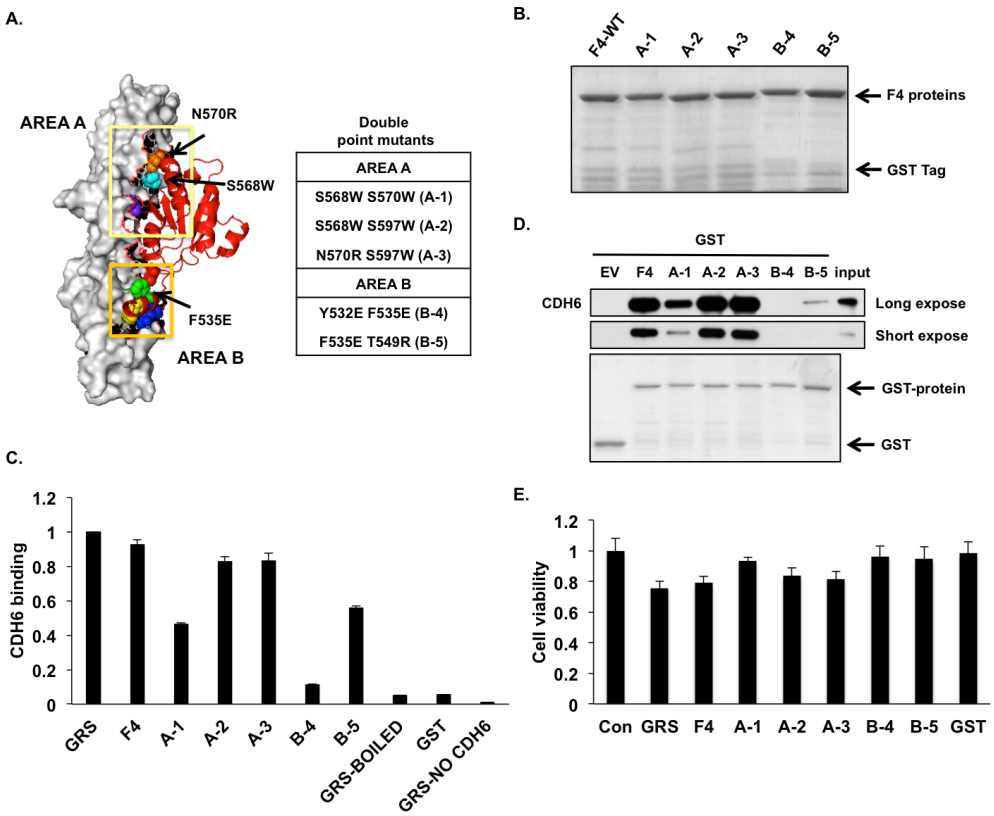

Figure 5. Double point mutation showing critical interaction between F4 and CDH6

(A) Using stringent mutant model, mutants docking area were divided into A and B. F535, S568, and N570 residues were used for the double point mutation within each area to see binding loss.

(B) F4 and double mutated mutants were purified to the purity was confirmed using Coomassie staining.

(C) Having GRS as positive control, F4 and double mutants were coated with 2 μg/ml and checked CDH6 (2 μg/ml) binding was tested using ELISA.

(D) Pull-down assay was used to confirm the CDH6 binding with double mutation. F4 and double mutants (4 μg) were used to test binding with CDH6 (2 μg) and 10% of CDH6 input was used for positive control. GST-empty

vector was used as negative control.

(E) CDH6 expressing cell line, H460, was treated with 100 nM of F4 and double mutants for 24 h and the cell viability was measured by CCK8 assay. GRS 100 nM was used as positive control to induce cell death.

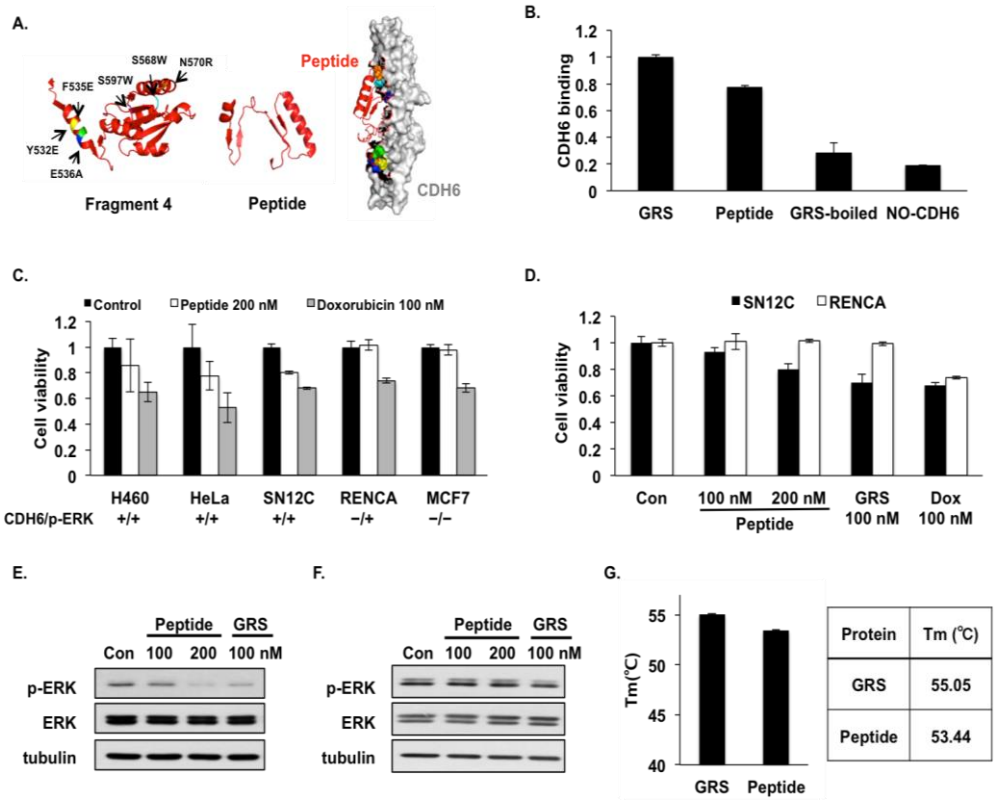

Figure 6. CDH6 binding and anti-tumor effects of peptide designed based on predicted active site domains.

(A) Peptide was designed including all stringent mutants residues. Peptide was designed to have alpha helix on both end and beta-sheet in inner area to maintain conformation. F4 fragment, peptide and peptide/CDH6 structures are shown.

(B) Peptide was coated with 2 μg/ml and checked CDH6 binding was tested using ELISA. GRS was used as a positive control.

(C) CDH6 and pERK positive or negative cell lines were used to check cell viability using peptide 200 nM to see CDH6 dependency. Doxorubicin 100 nM was used as a positive control.

(D) CDH6 positive renal cancer cell (SN12C) and CDH6 negative cell (RENCA)

were used to check viability in dose dependent manner.

(E) SN12C CDH6 positive cell line was used to check dephosphorylation of pERK using 100 nM and 200 nM of peptide. GRS 100 nM was used as a positive control.

(F) RENCA CDH6 negative cell line was used to check dephosphorylation of pERK using 100 nM and 200 nM of peptide. GRS 100 nM was used as a positive control.

(G) GRS and peptide Tm was measured using thermal shift assay.

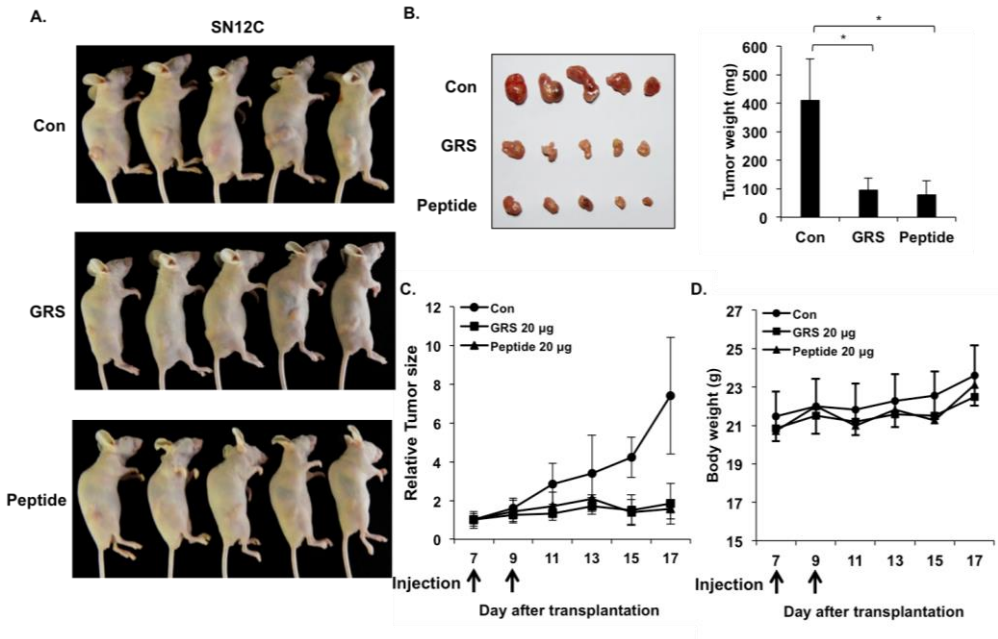

Figure 7. Peptide induces tumor regression in CDH6 positive cancer cell *in vivo*

(A) Photographs of SN12C xenograft tumor mice of PBS, GRS and peptide treated on day 7 and day 9 and monitored for 10 days.

(B) Photograph of tumor and weight were measured on the last day.

(C) CDH6 positive cells, SN12C, were subcutaneously injected into the BALB/c nude mice and grown for 7 days until average tumor size reach 100 mm^3. PBS, GRS (20 μg) and Peptide (20 μg) were intra-tumor injected (n=5 animal/group) day 7 and 9. Tumor volume was calculated as the longest diameter x the shortest $diameter^2$ x 0.52.

(D) The body weights were measured for Control, GRS and peptide after first day of protein injection.

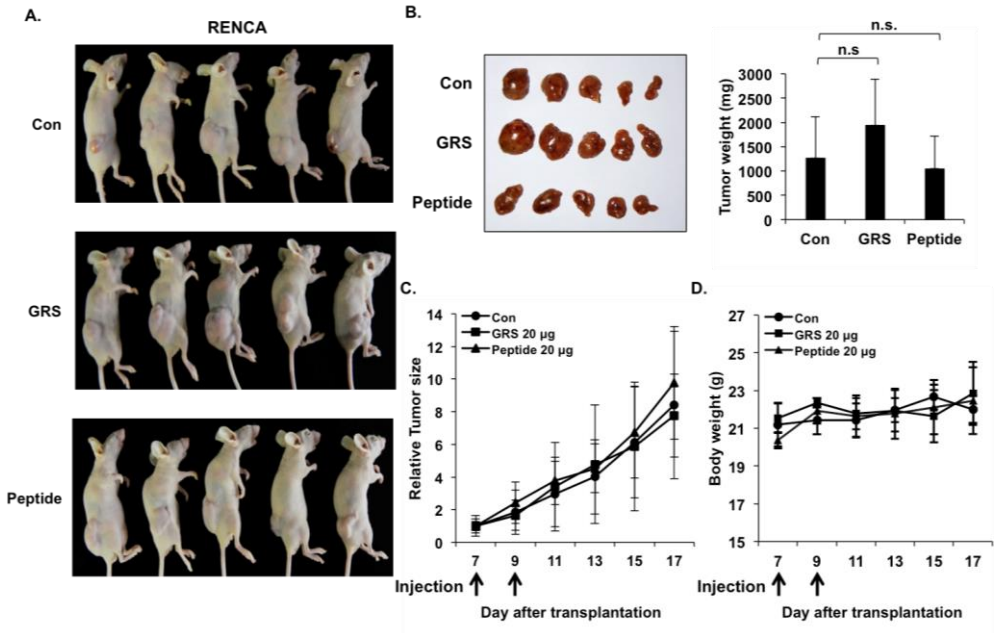

Figure 8. Peptide has no effect in CDH6 negative cancer cell *in vivo*

(A) Photographs of RENCA xenograft tumor mice of PBS, GRS and peptide treated on day 7 and day 9 and monitored for 10 days.

(B) Photograph of tumor and weight were measured on the last day.

(C) CDH6 negative cells, RENCA, were subcutaneously injected into the BALB/c nude mice and grown for 7 days until average tumor size reach 100 mm^3. PBS, GRS (20 µg) and Peptide (20 µg) were intra-tumor injected (n=5 animal/group) day 7 and 9. Tumor volume was calculated as the longest diameter x the shortest $diameter^2$ x 0.52.

(D) The body weights were measured for Control, GRS and peptide after first day of protein injection.

DISCUSSION

Peptides are up-rising alternative targeting agents for human cancers (1). Peptide can resolve the problems that antibodies are facing, such as large size and nonspecific uptake by the reticuloendothelial system and liver (17). Antibodies are used for blocking the signal in cancer therapy, but peptides are used to activate signaling pathway through receptor binding. Development of peptides that activate the signal pathways by blocking tumor growth or inducing apoptosis can be a strategy used for cancer therapy (18). Peptide targeting cancer has been approved by Food and Drug administration (FDA) for past few years (2). Octreotide, a first approved peptide targeting somatostain receptor have been used for treating acromegaly and symptoms in cancer patient. Since then, more than 60 peptide drugs have been approved by FDA and more than 140 peptide drugs are in clinical trials (19). Therefore, targeting cancer using peptide can minimize side effects and can be beneficial for therapeutic drug development.

GRS has been shown to have an anti-tumor effect through CDH6 binding by dephosphorylation of ERK. Therefore, finding CDH6 binding domain of GRS is important for development of peptide drug targeting CDH6/PP2A/ERK axis for cancer therapy (7). GRS binding receptor Cadherin-6, type II classical cadherin family, have been found preferentially expressed in kidney. Kidney cancer expresses higher level of CDH6 compare to normal (12, 20). Recently, antibody drug conjugate (ADC) targeting CDH6 for having high expression level in renal cancer are in clinical trial for targeting renal cancer drug (21). The drug development targeting renal cancer using CDH6 can be effective having high expression of CDH6 compare

to normal.

For therapeutic peptide development, anti-tumor or pro-tumor protein has been developed into peptide. Peptide derived from EGFR, P53, Bcl-2 and CXC chemokine is being developed into anti-tumor peptide for cancer treatment (22, 23). P53-derived peptide has been developed in order to induce necrosis of cancer cell developing mdm-2 binding site inducing mdm-2 and P53 competition and CKC chemokine derived peptide blocks basic components of angiogenesis (24, 25). Therefore, developing GRS binding domain into peptide for inducing cancer cell apoptosis through CDH6 binding. We decided to develop GRS-derived peptide having anti-tumor activity for the development of renal cancer therapeutic drug.

To determine CDH6 binding domain, GRS was divided into four fragments maintaining all existing domain and only fragment 4 (F4) showed CDH6 binding and anti-tumor activities *in vitro* and *in vivo*. Due to F4 poor stability, N-terminal of F4 inserted area of GRS and F4 fragment with different length of N-terminal truncated forms were designed in order to increase stability (26). As N-terminal gets truncated, the activity of F4 decreased. These results gave an idea that the CDH6 binding domain may exist around N-terminal region of F4. To delineate the CDH6 binding domain, potential docking interface of CDH6/F4 complex were predicted using Haddock 2.2 (14). Predicted binding residues were mutated and F535, S568 and N570 residues showed loss of CDH6 binding and activity. For confirm binding domain, double point mutation was performed to increase disruption in CDH6 binding and F535 residue has been found to be critical for CDH6 binding.

Based on the docking model prediction, peptide was developed having alpha helix segment on both ends and beta-strand-loop-beta strand to maintain

stability and conformation (27, 28). Peptide showed CDH6 binding and CDH6 dependent anti-tumor effects in dose dependent manner through dephosphorylation of ERK signal. Through mouse xenograft model, peptide showed tumor regression effect only toward CDH6 positive renal cancer cell. As a result, GRS-derived peptide showed binding toward CDH6 and anti-tumor effect toward renal cancer cell *in vitro* and *in vivo*.

GRS-derived peptide has high possibility for renal cancer therapeutic drug development. Current cancer treatments are chemotherapy and/or radiation therapy, but the side effects caused by immune response or non-specific treatments limit the effectiveness of the cancer therapy (29, 30). Peptides have low toxicity and the ability to bind to different receptor for activating anti-tumor signaling are being magnified for the promising therapeutic drug (31). Renal cell cancer (RCC) is known for aggressive cancer that arises from the proximal renal tubular epithelium of the kidney and there are no specific RCC targeting drug (32). GRS-derived peptide can be used for the RCC specific targeting drug, having anti-tumor effect through binding to CDH6, which is highly expressed in renal cell cancer. Peptide can be used for the RCC therapeutic drug having CDH6 specificity and advantage of low toxicity of peptide.

In this study, full length GRS was developed into 70 amino acids peptide sustaining anti-tumor effect by binding to CDH6 through dephosphorylation of ERK signaling. Also, we have shown the GRS peptide *in vivo* suppressed CDH6-positive tumor growth with low toxicity. This shows that GRS peptide is good drug candidate for cancers expressing CDH6.

REFERENCES

1. Craik DJ, Fairlie DP, Liras S, & Price D (2013) The future of peptide-based drugs. *Chem Biol Drug Des* 81(1):136-147.
2. Adare A*, et al.* (2011) Measurements of higher order flow harmonics in Au+Au collisions at radicals(NN)=200 GeV. *Phys Rev Lett* 107(25):252301.
3. Kaspar AA & Reichert JM (2013) Future directions for peptide therapeutics development. *Drug Discov Today* 18(17-18):807-817.
4. Guo M, Yang XL, & Schimmel P (2010) New functions of aminoacyl-tRNA synthetases beyond translation. *Nat Rev Mol Cell Biol* 11(9):668-674.
5. Kim S, You S, & Hwang D (2011) Aminoacyl-tRNA synthetases and tumorigenesis: more than housekeeping. *Nat Rev Cancer* 11(10):708-718.
6. Wakasugi K & Schimmel P (1999) Two distinct cytokines released from a human aminoacyl-tRNA synthetase. *Science* 284(5411):147-151.
7. Park MC*, et al.* (2012) Secreted human glycyl-tRNA synthetase implicated in defense against ERK-activated tumorigenesis. *Proc Natl Acad Sci U S A* 109(11):E640-647.
8. Chitaev NA & Troyanovsky SM (1997) Direct Ca2+-dependent heterophilic interaction between desmosomal cadherins, desmoglein and desmocollin, contributes to cell-cell adhesion. *J Cell Biol* 138(1):193-201.
9. Wheelock MJ & Johnson KR (2003) Cadherin-mediated cellular signaling. *Curr Opin Cell Biol* 15(5):509-514.
10. Nollet F, Kools P, & van Roy F (2000) Phylogenetic analysis of the cadherin superfamily allows identification of six major subfamilies besides several solitary

members. *J Mol Biol* 299(3):551-572.

11. Angst BD, Marcozzi C, & Magee AI (2001) The cadherin superfamily: diversity in form and function. *J Cell Sci* 114(Pt 4):629-641.

12. Patel SD, Chen CP, Bahna F, Honig B, & Shapiro L (2003) Cadherin-mediated cell-cell adhesion: sticking together as a family. *Curr Opin Struct Biol* 13(6):690-698.

13. Zuiderweg ER (2002) Mapping protein-protein interactions in solution by NMR spectroscopy. *Biochemistry* 41(1):1-7.

14. Dominguez C, Boelens R, & Bonvin AM (2003) HADDOCK: a protein-protein docking approach based on biochemical or biophysical information. *J Am Chem Soc* 125(7):1731-1737.

15. Fiser A, Do RK, & Sali A (2000) Modeling of loops in protein structures. *Protein Sci* 9(9):1753-1773.

16. D. A. Case VB, J. T. Berryman, et al. (2014) *Amber 14*.

17. Chames P, Van Regenmortel M, Weiss E, & Baty D (2009) Therapeutic antibodies: successes, limitations and hopes for the future. *Br J Pharmacol* 157(2):220-233.

18. Boohaker RJ, Lee MW, Vishnubhotla P, Perez JM, & Khaled AR (2012) The use of therapeutic peptides to target and to kill cancer cells. *Curr Med Chem* 19(22):3794-3804.

19. Fosgerau K & Hoffmann T (2015) Peptide therapeutics: current status and future directions. *Drug Discov Today* 20(1):122-128.

20. Paul R*, et al.* (1997) Cadherin-6, a cell adhesion molecule specifically expressed in the proximal renal tubule and renal cell carcinoma. *Cancer Res* 57(13):2741-2748.

21. Bialucha CU*, et al.* (2017) Discovery and Optimization of HKT288, a Cadherin-6 Targeting ADC for the Treatment of Ovarian and Renal Cancer. *Cancer Discov*.

22. Kolluri SK, *et al.* (2008) A short Nur77-derived peptide converts Bcl-2 from a protector to a killer. *Cancer Cell* 14(4):285-298.

23. Ofuji K, *et al.* (2015) A peptide antigen derived from EGFR T790M is immunogenic in non-small cell lung cancer. *International Journal of Oncology* 46(2):497-504.

24. Michl J, *et al.* (2006) PNC-28, a p53-derived peptide that is cytotoxic to cancer cells, blocks pancreatic cancer cell growth in vivo. *Int J Cancer* 119(7):1577-1585.

25. Karagiannis ED & Popel AS (2008) Novel anti-angiogenic peptides derived from ELR-containing CXC chemokines. *J Cell Biochem* 104(4):1356-1363.

26. Lu Z, Wang Q, Jiang S, Zhang G, & Ma Y (2016) Truncation of the unique N-terminal domain improved the thermos-stability and specific activity of alkaline alpha-amylase Amy703. *Sci Rep* 6:22465.

27. Errington N, Iqbalsyah T, & Doig AJ (2006) Structure and stability of the alpha-helix: lessons for design. *Methods Mol Biol* 340:3-26.

28. Doig AJ & Baldwin RL (1995) N- and C-capping preferences for all 20 amino acids in alpha-helical peptides. *Protein Sci* 4(7):1325-1336.

29. Luo Y & Prestwich GD (2002) Cancer-targeted polymeric drugs. *Curr Cancer Drug Targets* 2(3):209-226.

30. Li C (2002) Poly(L-glutamic acid)--anticancer drug conjugates. *Adv Drug Deliv Rev* 54(5):695-713.

31. Xiao YF, *et al.* (2015) Peptide-Based Treatment: A Promising Cancer Therapy. *J Immunol Res* 2015:761820.

32. Gupta K, Miller JD, Li JZ, Russell MW, & Charbonneau C (2008) Epidemiologic and socioeconomic burden of metastatic renal cell carcinoma (mRCC): a literature review. *Cancer Treat Rev* 34(3):193-205.

33. Zhang Q, Zeng SX, & Lu H (2015) Determination of Maximum Tolerated Dose and Toxicity of Inauhzin in Mice. *Toxicol Rep* 2:546-554.

요약 (국문초록)

항암 치료를 위한

Glycyl-tRNA synthetase 유래 Peptide 개발

서울대학교
융합과학기술대학원
분자의학 및 바이오제약학과 의약생명과학전공
박찬호

펩티드 의약품은 새로 주목받고 있는 항암제이다. 펩티드는 빠르게 합성이 가능하고 특정 부분을 쉽게 변경할 수 있기 때문에 약물 전달 시스템에 용이하게 적용할 수 있다. 화학 물질 보다 펩티드는 독성이 적고, 부작용이 낮아 의약품으로서 활발한 연구가 진행되고 있다. Glycyl-tRNA synthetase (GRS)는 번역과정에 관여하는 단백질로 알려져 있지만, 이외에도 인체 내에서 다양한 기능을 하는 것으로 보고되고 있다. 기존에 GRS가 CDH6 (K-cadherin) 라고 알려진 수용기와 반응함으로써, CDH6와 결합하고 있는 PP2A가 떨어져 나가게 하여 ERK를 탈인산화시켜 ERK 활성을 억제함으로써 세포 사멸을 유도한다고 알려져 있다. CDH6와 결합하는 GRS의 결합 부분을 찾기 위해서, GRS를 4개의 절편으로 나누어 CDH6 결합력 및 항암효과를 분석하였다. F4라는 네번째 절편이 CDH6와 결합하고 암세포 사멸을 유도하는 것을 확인하였다. CDH6와 결합하지 않는 F2 절편과 CDH6와 결합하는 F4 절편을 이용하여 이종이식 실험을 진행하였을 때, CDH6와 결합하는 F4 절편만이 종양 감소를 보였다. High ambiguity Driven protein-protein DOCKing (Haddock 2.2)라는 프로그램을 이용

하여, F4 절편과 CDH6가 가장 안정적으로 결합하는 부위를 예측하였다. 활성부위를 규명하기 위하여, 결합하는 잔기를 점 돌연변이 시켜 항암활성과 CDH6와의 결합이 줄어드는지를 확인하였다. 가능성이 있는 잔기 주변을 기존 잔기와 상반되는 아미노산으로 바꾸었을 경우, 결합이나 항암활성이 줄어드는 것을 F535, S568 그리고 S570의 잔기에서 확인하였다. 이들 잔기에 이중 돌연변이를 만들어 CDH6 결합과 항암활성을 확인한 결과 F535를 포함하는 이중 돌연변이들에게서 극적인 결합 감소를 관찰하였다. 이 결과를 토대로 예측 결합 잔기들을 모두 포함하는 펩티드를 제작하여 펩티드가 CDH6와 결합하고 CDH6에 의존적으로 항암 효과를 보이는 것을 세포 및 이종이식 모델에서 확인하였다. 본 연구결과는 GRS의 CDH6 결합 영역을 규명하여 이를 토대로 항암활성을 가진 기능성 펩티드 의약품을 개발할 수 있는 가능성을 제시하였다.

주요어 : Glycyl-tRNA synthetase, 펩티드, HADDOCK 2.2 , 의약품, CDH6, 돌연변이 유발, 아미노산

학 번 : 2015-26077